Int. J. Electrochem. Sci., 16 **(2021)** Article ID: 21029, doi: 10.20964/2021.02.09

International Journal of
ELECTROCHEMICAL
SCIENCE
www.electrochemsci.org

Effect of Cr-C Coatings on the Corrosion Resistance of 304 Stainless Steel in the Molten Sodium Polysulfide

Yanjie Ren[1,*], *Chenyang Du*[1], *HuayueDu*[1], *Jian Chen*[1], *Yuhang Zhao*[2,*]

[1] School of Energy and Power Engineering, Changsha University of Science & Technology, Changsha, Hunan 410114, China
[2] Research Center of ShenHua Zhunneng Comprehensive Resource Development Co. Ltd, Ordos, 010300, China
[*]E-mail: yjren@csust.edu.cn (Yanjie Ren), yuhangzhao8310@163.com (Yuhang Zhao)

Received: 16 September 2020/ *Accepted:* 6 November 2020 / *Published:* 31 December 2020

The corrosion of metallic containers in Na-S batteries cause an increase in resistance, a loss of battery capacity and cycling life limitations. In this paper, a Cr-C coating was deposited on 304 stainless steel by a direct current magnetron sputtering technique. XRD analysis showed that the as-deposited Cr-C coating mainly consisted of Cr_3C_2, Cr_7C_3 and Cr. After corroding in molten sodium polysulfide at 350°C for 100 h, $NaCrS_2$ and Cr_2S_3 were generated on the surface of the coating. The charge transfer resistance of this Cr-C coating was higher than that of 304SS by approximately 3 orders of magnitude, showing improved corrosion resistance.

Keywords: Sodium sulfur batteries; Container; Cr-C coating; Electrochemical corrosion behaviour; Direct current magnetron sputtering

1. INTRODUCTION

In recent years, sodium-sulfur batteries have developed rapidly due to their advantages, such as their high energy density, high power density, and low self-discharge rate[1-2]. In Na-S batteries, a metallic container is used to encase the mixture of molten sulfur and sodium polysulfides at 350°C. Moreover, the container also serves as the final current collector for the sulfur side. However, the container/current collector inevitably suffers severe corrosion in the highly corrosive molten polysulfide, resulting in the loss of capacity, increase in resistance and cycling life limitations[3-5]. Thus, the container must simultaneously satisfy the requirements of corrosion resistance and electrical conductivity to resist the attack of highly corrosive molten sulfur and sodium polysulfides. Some metals, such as chromium, molybdenum and tungsten, have been examined as candidate materials for containers of Na-S batteries[6-8]. Among them, only molybdenum is supposed to exhibit excellent corrosion resistance and electrical conductivity. However, its high cost and poor charge transfer characteristics

make it unacceptable for practical application[6].

To solve this problem, some candidate coating materials, e.g., molybdenum, Ni-W, perovskite oxides, carbon, and chromium-rich diffusion coatings or conducting ceramics, have been examined[9-12]. Zhang et al observed that an amorphous Ni-W coating could improve the corrosion resistance of SS430 in a molten sulfur environment while also improving the conductivity. Huang et al synthesized perovskite $La_{0.8}Sr_{0.2}Co_{0.2}Cr_{0.8}O_{3-\delta}$ (LSCC) ceramic coatings on stainless steel current collectors for use in Na/S batteries by the conventional ceramic processing technique and found that these LSCC coatings showed excellent corrosion resistance in molten sodium tetrasulfide at 350°C.

Chromium carbide has been claimed to have excellent corrosion resistance in air and supercritical water[13]. Chromium carbide coatings are easily deposited by the magnetron sputtering technique, and the obtained Cr-C systems contain several crystalline phases with complex structures[14-15]. The corrosion behaviour of Cr-C films in sodium polysulfides has not previously been documented in any significant detail. In this paper, a chromium carbide film was deposited on the surface of 304SS by the magnetron sputtering method, and its corrosion resistance in a molten polysulfide was investigated by electrochemical impedance spectroscopy. The aim is to evaluate the resistance of Cr-C-coated metallic containers against molten polysulfide corrosion in Na-S batteries.

2. EXPERIMENTAL

2.1 Preparation of the Cr-C coatings

The Cr-C films herein were prepared by direct current magnetron sputtering with bulk Cr_3C_2 (99.9%) as the target. During deposition, the base pressure was $3*10^{-3}$ Pa, the working pressure was 0.5 Pa, and the substrate temperature was 500°C. The target power was 150 W. The target was pre-sputtered for 15 min before each sputtering to achieve a stable sputtering state.

2.2 Electrochemical impedance measurements

A two-electrode system was used for electrochemical impedance measurements. The bare 304SS and as-deposited chromium carbide-coated 304SS samples were used as the working electrodes in the electrochemical measurements. These electrodes were prepared as follows: Fe-Cr wires were spot-welded to one end of the bare or chromium carbide-coated 304SS samples for the electrical connection. Two closely spaced samples were sealed in alumina tubes with high-temperature cement. The cement was dried at room temperature and then solidified at 100°C for 24 h and 350°C for 10 h.

Sodium sulfide was dried in a vacuum drying oven and then mixed with sulfur powder at a molar proportion of 1:4. The electrode was dipped into the melt for 120 h, and electrochemical impedance spectroscopy (EIS) was used to study the corrosion behaviour of chromium carbide-coated 304SS. EIS measurements were performed at open-circuit potential between 0.01 and 1×10^5 Hz using a Zahner potentiostat(Zennium model) with an amplitude of 5 mV for the input sine signal. The samples after corrosion in the molten sodium polysulfide were characterized by scanning electron microscopy (SEM) and X-ray diffraction (XRD).

3. RESULTS AND DISCUSSION

3.1 Composition and microstructural analysis of the as-deposited chromium carbide coatings

Figure 1 shows the morphology and grazing incidence X-ray diffractogram of the as-deposited Cr-C coatings by magnetron sputtering. Depending on the deposition parameters, the Cr-C films prepared by magnetron sputtering are composed of amorphous, polycrystalline, or a mixture of nanocrystalline carbide particles[16-18]. Herein, the as-deposited Cr-C coating exhibited a cauliflower-like structure, and the grain size is approximately 50-100 nm. As shown in Fig. 1 b, the as-deposited chromium carbide coating consists of Cr_3C_2, Cr_7C_3 and Cr. Similarly, Nygren observed that Cr was available at 300°C for Cr-C films deposited by non-reactive magnetron sputtering[16].

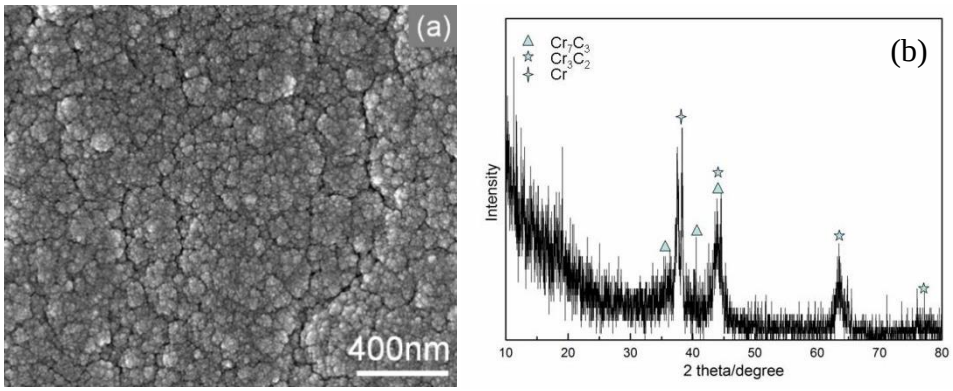

Figure 1. (a)Surface morphology (b) XRD image of as-deposited Cr-C coating by direct current magnetron sputtering

Figure 2 shows the AFM image of the chromium carbide film deposited by direct current magnetron sputtering, where R_{max} (the distance between the highest and lowest points) is 652 nm, and Image R_{max} (roughness) is 91.5 nm, indicating that the as-deposited chromium carbide coating is uniform.

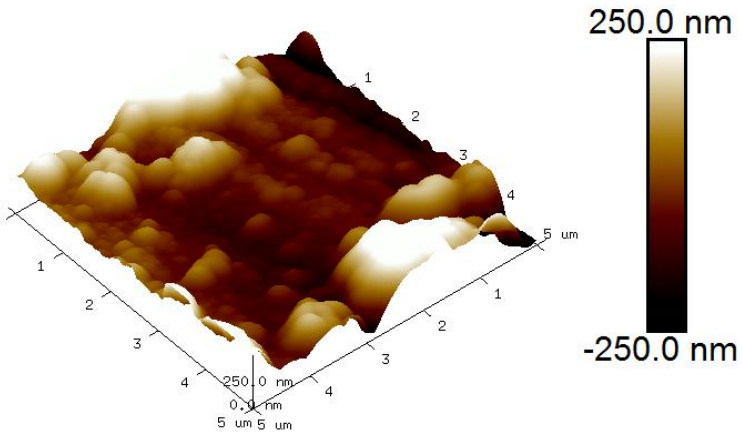

Figure 2. AFM image of the Cr-C coating deposited by direct current magnetron sputtering

3.2 Electrochemical Corrosion Behaviours of Chromium Carbide Coated 304SS

The electrochemical impedance technique was employed to investigate the corrosion behaviour of bare 304SS and Cr-C-coated 304SS in molten sodium polysulfide. The typical impedance spectroscopy of 304SS corroded in molten sodium polysulfide for 96 h is shown in Figure 3. It can be seen that the impedance spectroscopy is composed of a small semicircle at high frequency and a straight line at low frequency, indicating that the process is controlled by the diffusion of species to the molten salt/substrate interface. The impedance behaviour of the bare 304SS is fitted using the equivalent electrical circuit (EEC) shown in Fig. 4, where Ra represents the anodic charge transfer resistance and Z_w is the Warburg resistance. Due to the dispersion effect, the electrochemical impedance Z can be expressed by the following equation[19]:

$$Z = R_s + \frac{1}{j\omega C_{dl} + \omega C_{dl}\cot(\beta\Pi/2) + \frac{1}{Ra} + \frac{1}{Z_w}}$$

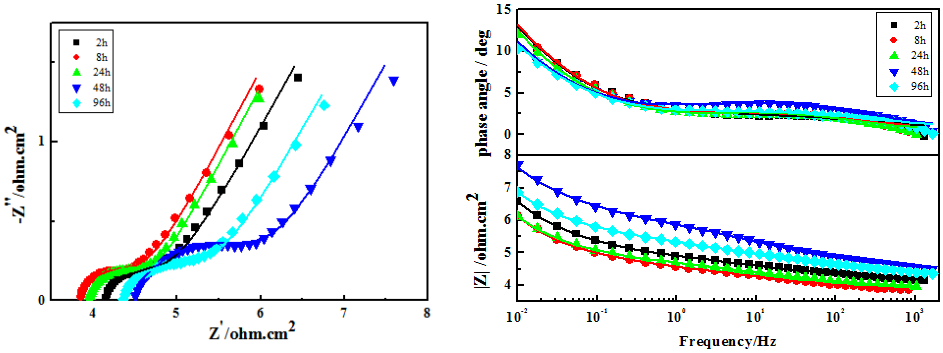

Figure 3. Nyquist and Bode plots for 304SS after various exposure times in molten sodium polysulfide

The fitted EIS parameters are shown in Table 1. The simulated impedance data are in good agreement with the experimental data, as shown in Fig.3.The fitted n_{dl} coefficient is always far less than 1, indicating a significant dispersion effect.

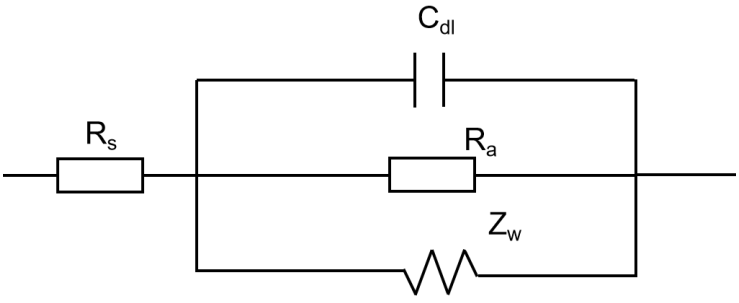

Figure 4. Equivalent circuit representing the corrosion of 304SS corroded in molten salts

Table 1. The fitted results of 304SS corroded in the molten polysulfide at 350℃

Time (h)	R_s ($\Omega.cm^2$)	Y_{dl} ($S^{-\alpha}\Omega^{-1}$ cm^{-2})	n_{dl}	R_a ($\Omega.cm^2$)	W ($S^{-0.5}\Omega$ cm^{-2})
2	4.026	0.183	0.376	1.144	1.590
24	3.904	0.110	0.515	0.857	2.053
48	4.384	0.088	0.432	1.897	1.823
96	4.225	0.155	0.365	1.517	1.899

Figure 5 shows the impedance spectrum of the Cr-.C-coated 304SS corroded in sodium polysulfide for 100 h. After immersion for 8 h, the Nyquist plot consists of only one capacitive loop in the impedance spectrum, indicating that the spectroscopy results only reflect the information of the Cr-C coating. After extending the immersion time, the spectra are composed of two indistinguishable capacitive loops. The capacitive loops contract after immersion for 24 h and then expand gradually from 65 to 100 h. Correspondingly, the phase angle in the low-frequency region and the impedance value increases, suggesting an improved corrosion resistance.

An equivalent circuit (Fig. 6 a) of the molten salt resistance Rs in series with a parallel circuit consisting of an interfacial capacitance C_f and an interfacial resistance R_f was proposed to fit the impedance spectroscopy of the Cr-C coatings corroded for 8 h. The impedance spectra of the Cr-C coating corroded for 24, 65 and 100 h in the polysulfide are represented by the EEC shown in Fig.6 b, where C_f correlates to the coating capacitance, R_f is the micropore resistance of the coating, C_{dl} is related to the double-layer capacitance at the coating/molten salts interface and R_t is charge transfer resistance between the coating and molten salts.

The fitted results are listed in Table 2. There is a significant drop in R_f from 1501.2 to 9.4287 $\Omega.cm^2$ between 8 and 24 h, which can be attributed to the diffusion of molten polysulfide along the microdefects in the Cr-C coating. Moreover, the active Cr in the coating can react with the molten sulfide and form chromium sulfide. From 24 to 100 h, R_t increases from 328.1 to 1182.3 $\Omega.cm^2$, suggesting that the transfer of charged ions at the coating/melt interface becomes more difficult. The formation of chromium sulfide along the microdefects of the coating contributes to the increase in film resistance R_f. After immersion for 100 h, the charge transfer resistance R_t value of the Cr-C coating is approximately 3 orders of magnitude higher than that of 304 stainless steel in molten sodium polysulfide, showing that the Cr-C coating can effectively suppress the corrosion of304SS in molten salt.

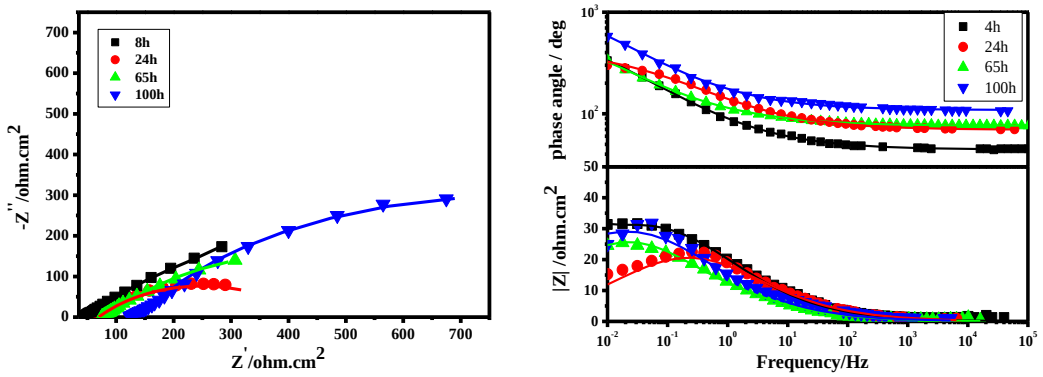

Figure 5. Nyquist and Bode plots for Cr-C coating after various exposure times in molten sodium polysulfide

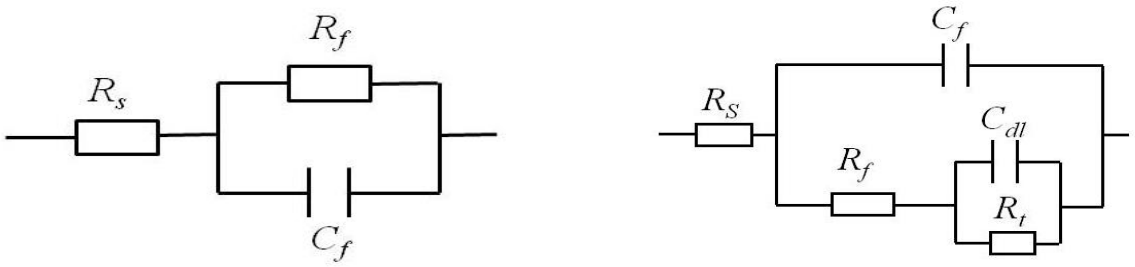

(a) (b)

Figure 6. Equivalent circuit representing the corrosion of Cr-C coated 304SS corroded for (a) 8h (b) 24h 65h and 100h in molten salts

Table 2. The fitted results of Cr-C coated 304SS corroded in the molten polysulfide at 350 ℃

Time (h)	R_s ($\Omega.cm^2$)	Y_f ($S^{-\alpha}\Omega^{-1}\,cm^{-2}$)	n_f	R_f ($\Omega.cm^2$)	Y_{dl} ($S^{-\alpha}\Omega^{-1}\,cm^{-2}$)	n_{dl}	R_t ($\Omega.cm^2$)
4	38.86	0.0109	0.4754	1501.2			
24	38.58	0.0104	0.4569	9.428	1.447E-4	0.4578	328.1
65	70.06	0.0091	0.5227	111.8	4.71E-3	0.5850	580.9
100	123.8	0.0037	0.4996	189.2	1.08E-3	0.7925	1182.3

Figure 7 shows the morphology of Cr-C coated 304SS corroded in molten sulfur polysulfide for 100 h. The Cr-C coating remains intact, and no delamination is observed in the Cr-C coating. Figure 8 shows the XRD analysis of Cr-C coated 304SS corroded for 100 h in molten sodium polysulfide. In

addition to the Cr_3C_7 and Cr_3C_2 phases, $NaCrS_2$ and Cr_2S_3 form due to the reaction of active Cr in the Cr-C coating.

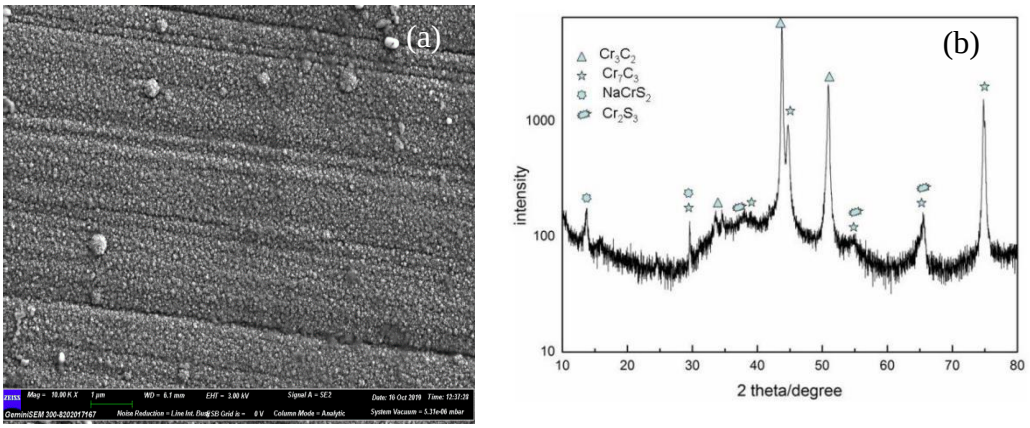

Figure 7. (a)Surface morphology (b)XRD image of Cr-C coating corroded in the molten polysulfide for 100h.

3.3. Proposed corrosion mechanism of 304SS and the Cr-C coating in molten sodium polysulfides

The electrochemical process of hot corrosion consists of a cathodic and anodic process. Differing from aqueous corrosion, the anodic dissolution of active metals in molten salt occurs easily, and the transport of ions in the scale and diffusion of oxidants in the melts may become rate-limiting processes[19]. In regard to 304SS in the molten polysulfide, the active Fe and Cr are apt to react rapidly with the polysulfide and form Na_3FeS_3 and $NaCrS_2$[12], and the diffusion of these molten sulfides to the scale/substrate interface is not enough to meet their consumption in the reaction. In this case, the anodic charge transfers are not rate-limiting, and the corrosion of the stainless steel is controlled by the diffusion of corrosive ions to the stainless steel/molten sodium polysulfide interface. Therefore, Nyquist plots of the bare steel in the molten polysulfide consist of a small capacitive loop in the high-frequency region and a line in the low-frequency region.

In contrast, for Cr-C-coated steel, chromium carbide is stable in the molten sodium polysulfides; therefore, at the initial stage, the impedance spectrum only reflects the characteristics of the film. However, after extending the immersion time, the molten salts diffuse along the Cr-C coating to the surface of steel and form Na_3FeS_3 and $NaCrS_2$ compounds. Moreover, the molten polysulfide can react with the active Cr distributed in the chromium carbide coatings and form chromium sulfide, such as Cr_3S_2. Chromium sulfide is stable in the molten salt and increases the chemical stability of the Cr-C coating. Furthermore, the formation of Cr_2S_3 and the corrosion product formed on the surface of the coating/steel can block the microdefects and inhibit the inward penetration of corrosive species. Similar results were also observed by Huang[11]. Thus, it can be observed that the coating resistance R_f and charge transfer resistance R_t increase from 24 to 100 h. Conclusively, the Cr-C coating can improve the corrosion resistance of 304SS in molten polysufide at 350°C. Looking towards the future, the variation in coating composition by controlling the deposition parameters and the effects of these compositions

on corrosion resistance over long-term immersion still needs further investigation, and related work is ongoing.

4. CONCLUSIONS

Cr-C coatings were deposited on 304 stainless steel by a direct current magnetron sputtering technique with the aim to enhance the resistance of the container against the corrosion of the molten polysulfide in Na-S batteries. Electrochemical methods were used to evaluate the corrosion resistance of the coating in molten sodium polysulfide at 350°C. The as-deposited Cr-C coating was dense and consisted of Cr_3C_2, Cr_7C_3 and Cr. In the case of bare 304SS, the corrosion of stainless steel was controlled by the diffusion of corrosion products to the stainless steel/molten sodium polysulfide interface. The R_t values remained at approximately 0.857~1.897 $\Omega.cm^2$, indicating that 304SS underwent fast corrosion in molten polysulfide. In regard to the Cr-C coating, after corroding in molten sodium polysulfide at 350°C for 100 h, the chromium carbide coating remained intact, and no delamination was observed. The charge transfer resistance R_{ct} for the Cr-C coating after immersion for 100 h was approximately 3 orders of magnitude higher than that of 304SS, indicating that the coating could improve the corrosion resistance of 304SS containers in Na-S batteries.

ACKNOWLEDGMENTS
This work was supported by the National Natural Science Foundation of China (No.51771034), National Natural Science Foundation of Hunan Province(No.2020JJ4610).

References

1. Z.Wen, J.Cao, X.H. Gu, X.U. Zhang and Z.Lin, *Solid State Ionics*, 179 (2008) 1697.
2. E.M.G. Rodrigues, G.J. Osório, R. Godina, A.W. Bizuayehu, J.M. Lujano-Rojas, J.C.O. Matias and J.P.S. Catalão, *Energy*, 90 (2015) 1606.
3. Z. Wen, Y. Hu and X. Wu, *Adv. Funct. Mater.,* 23 (2017) 1005.
4. R.Okuyama, H. Nakashima, T. Sano and E. Nomura, *J. Power Sources*, 93 (2001) 50-54.
5. Z. Yang, J. Zhang and M.C. Kintner-meyer, *Chem. Rev.,* 111 (2011) 3577.
6. P. Alan Brown, *J. Electrochem. Soc.*, 134 (1987) 1921.
7. R. Knodler, *J. Appl. Electrochem.,* 18 (1988) 653.
8. K. Jung, H. Heo, J. Lee, Y. Park and C. Kang, *Corros. Sci*., 98 (2015) 748.
9. M.F. Zhang, C.F. Zhu, C.P. Yang and Y.N. Lv, *Surf. Coat. Technol.*, 346 (2018) 40.
10. Y. Huang, Z. Wen, J. Yang, J. Cao and Y. Liu, *Electrochim. Acta*, 55 (2010) 8632.
11. Y. Huang, Z. Wen, J. Yang, J. Cao and Y. Liu, *Solid State Ionics*, 192 (2011) 364.
12. D. S. Park and D. Chatterji, *Thin Solid Films*, 83 (1981) 429.
13. S. Sahoo, S.K. Pradhan, M. Jeevitha, S. Bagchi and P.K. Barhai, *J. Non-Cryst. Solids*, 386 (2014) 14.
14. D. Martínez-Martínez, C. López-Cartes, A. Fernández and J.C. Sánchez-López. *Thin Solid Films*, 517 (2009) 1662.
15. J. Högström, M. Andersson, U. Jansson, F. Björefors and L. Nyholm, *Electrochim. Acta*, 122 (2014) 224.
16. A. Jellad, S. Labdi and T. Benameur, *J. Alloys Compd.*, 483 (2009) 464.

17. A. Jellad, S. Labdi, C. Malibert and G. Renou, *Wear*, 264 (2008) 893.
18. M. Andersson, J. Högström, S. Urbonaite, A. Furlan, L. Nyholm and U. Jansson, *Vacuum*, 86 (2012) 1408.
19. C.L. Zeng, W. Wang and W.T. Wu, *Corros. Sci.*, 43 (2001) 787–801